Al-Khwarizmi Engineering Journal, Vol. 19, No. 2, June, (2023)
P. P. 26- 38

Al-Khwarizmi Engineering Journal

Removal of Malachite Green from Aqueous Solution using Ficus Benjamina Activated Carbon-Nonmetal Oxide synthesized by pyro Carbonic Acid Microwave

Khatab Emad Talib* **Sami D. Salman****

*,**Department of Biochemical Engineering/ Al-Khwarizmi College of Engineering/ University of Baghdad/ Baghdad/ Iraq

*Email: khattab.i@kecbu.uobaghdad.edu.iq

**Email: sami.albayati@gmail.com

(Received 20 December 2022; accepted 8 March 2023)

https://doi.org/10.22153/kej.2023.03.002

Abstract

Activated carbon derived from Ficus Binjamina agro-waste synthesized by pyro carbonic acid microwave method and treated with silicon oxide (SiO2) was used to enhance the adsorption capability of the malachite green (MG) dye. Three factors of concentration of dye, time of mixing, and the amount of activated carbon with four levels were used to investigate their effect on the MG removal efficiency. The results show that 0.4 g/L dosage, 80 mg/L dye concentration, and 40 min adsorption duration were found as an optimum conditions for 99.13% removal efficiency. The results also reveal that Freundlich isotherm and the pseudo-second-order kinetic models were the best models to describe the equilibrium adsorption data.

Keywords: *Ficus Benjamina activated carbon; Microwave irradiation; Taguchi experiment*.

1. Introduction

Freshwater in particular and water, in general, have become more necessary during the past few years as a dearth of fresh water has been observed largely, as the expansion of the industrial sector in general and human expansion has led to the scarcity of water and increased demand for fresh water. [1,[2] 2]. Industrial expansion and human expansion have increased the need for clean water as this expansion has increased the proportion of effluents and increased the use of fertilizers and other substances that adversely affect the purity and cleanliness of the water and cause significant water pollution [3][4]. In industries in general, effluents and other wastes are often dumped without being processed to water sources from rivers and lakes, where they have been contaminated, where they need to be chemically treated and used again industrially [5,6].

In the last decade, the treatment of sewage has been of great importance, as dyes that change the color of the water are one of the chemicals that industrial discharges release. [7,8]. Since the presence of the least concentration of toxic dyes in water has serious consequences for the environment, dyes are often disposed of in the pharmaceutical, cosmetic, food, textile, leather, printing, and paper industries. [9,10]. Textile industries contribute to the largest pollution of dyes due to their ineffectiveness because dye molecules are not fully related to fabrics or tissues, where the majority of dye residues in textile industries are disposed into the environment[11,12].

Dyes disposed of from industries in general and textile industries, in particular, have attracted great attention because of the effects they cause, as there are a large number of harmful chemicals that make up dyes that are presented as liquid residues to factories, and these chemicals will contaminate

water and cause damage to the aquatic environment[13,14].

Dyes affect photosynthesis processes where they block sunlight and prevent it from penetrating the layers of water to reach aquatic organisms and plants, in addition to the impact of these toxic chemicals resulting from dyes on human and animal health. [15,16].

Annually large quantities and different types of dyes are produced and used in industry in general. Mg dye is an organic dye with cationic basic which is often used in paper and pharmaceutical industries, leather and textile industries, and food industries as food coloring, and food additives and also used in other applications such as its use as a fungal and parasitic pesticide in the field of aquaculture as well as anthelminthic[17,18].

In addition to all these uses for dyeing mg, many studies have revealed the dangerous and toxic effects of the use of mg dye, as it is toxic to aquatic organisms because of the presence of strong metal ions, which tend to increase their toxicity to aquatic organisms as well as show that they affect plants where the roots of plants absorb water contaminated with mg dye where they affect metabolism. Teratological, carcinogenic threats, and mutagenic threats are considered untreated mg dye from one of their causes, affecting the food chain by entering and accumulating dye molecules in the food chain, leading to the aforementioned threats to mammalian cells[19]. Other unwanted impacts incorporate side effects on the liver, and spleen, heart harm, skin injuries, lessening in fertility rates, growth rate, and development. Despite this, they too act as a tumor promoters in liver cells by diminishing malachite green, expanding its perseverance, and actuating apoptosis and tumor. Hence, there's prime significance within the removal or treatment of MG color profluent due to its poisonous impacts on the biological system[20,21]. There are many methods used to remove dyes and these methods used are coagulation, electrochemical oxidation, membrane filtration, rhizoremediation, ozonation, reverse osmosis, Flocculation, precipitation, adsorption, phytoremediation, and ultrasonication [22,23]

Of all the methods mentioned, the adsorption method is the most appropriate and has attracted researchers among the previous methods to use it in the purification of unprocessed water for the following reasons in terms of operational cost and removal of complex organic structures as well as in terms of the least productive of byproducts [24].

A nonreactive, equilibrium technique that includes particle accumulation on the two-section interface is known as adsorption [25]. Being fee-effective, easy operation, and quite efficient, the adsorption method is extensively used for the removal of poisonous dyes from the tainted environment [26 27]. Also, the overall performance of adsorptive separation improves with the traits of the adsorbent [28]. Properties together with the terror group, floor area, nontoxicity, reusability, and a fee of the adsorbent are of paramount significance withinside the dye expulsion from business effluents[29,30]. Different adsorbents exploited for MG dye adsorption consist of nylon microplastics[31], almond gum [32], litchi peel biochar [33], calcium alginate nanoparticles [34], Avena sativa hull [35], brewer's spent grain[36], nanocomposites[37], and clayey soil [38]. In a few cases, the expensiveness of activated carbon organized from various substances limits its utilization withinside the dye elimination technique. Hence, little research was done on the soil as an adsorbent, for example, floor soils [39] and Laterite soil [40].

This study focused on the use of activated carbon derived from Ficus Binjamina agro-waste synthesized by pyro carbonic acid microwave method and treated with silicon oxide (SiO_2) to produce AC/SiO_2 composite precursor to remove MG produce dye from aqueous solution. Batch adsorption was utilized to investigate the effect of three factors with four variables of concentration of dye, mixing time, and the amount of adsorbent on the removal efficiency.

2. Experimental

2.1. Adsorbate Preparation

Malachite Green (MG) dye stock at various concentrations was prepared from a standard solution of MG dye by dissolving 1 g of MG dye in 1 L of distilled water. The standard solution was diluted with distilled water to achieve the desired dye solution concentrations (20 – 80) mg/L. The various concentration of dye was determined using UV-visible spectroscopy with a calibration curve as illustrated in Figure 1.

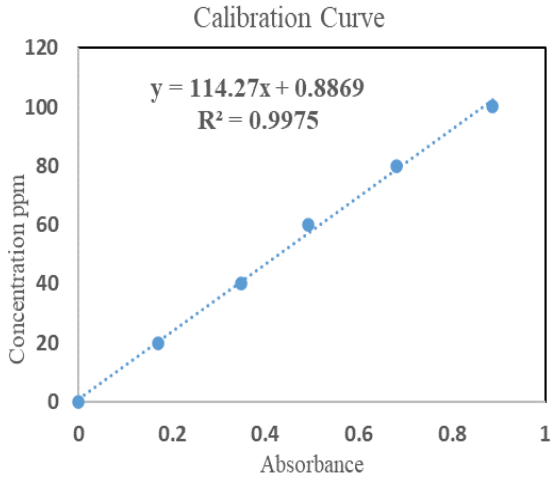

Fig.1. Calibration Curve of MG concentration.

3.1 Experimental Design

In this study, three independent factors with four levels of initial dye concentration, mixing time, and adsorbent dosage were selected for design experiments as shown in Table 1, whereas and Taguchi method with 16 experiments was generated by STATISTICA 12.5 Software to investigate their impact on the quality of MG dye adsorption as shown in Table 2.

Table 1,
Factors with their levels of Taguchi design method.

Parameter	Factor	Level			
MG concentration (ppm)	X_1	20	40	60	80
Mixing time (min)	X_2	20	40	60	100
Dose of AC (g/L)	X_3	0.10	0.20	0.30	0.40

Table 2,
Number of runs proposed by the Taguchi method

Ci (ppm)	Time (min)	Dosage (g/L)
20	20	0.1
20	40	0.2
20	60	0.3
20	100	0.4
40	20	0.4
40	40	0.3
40	60	0.2
40	100	0.1
60	20	0.2
60	40	0.1
60	60	0.4
60	100	0.3
80	20	0.3
80	40	0.4
80	60	0.1
80	100	0.2

3.1 Adsorbent Preparation and Characterization

The composite adsorbent was prepared (AC-SiO2) was prepared from Ficus Benjamin twigs collected from the gardens of the university of Baghdad. The twigs were firstly washed with water to remove dust and dried overnight in an oven at 100 degrees Celsius. The dried twigs were crushed and sieved through a mesh sieve (720 micrometer-1mm), then the sample was impregnated at high temperatures, sio2 powder (30nm) was impregnated in 60% H3PO4 impregnated time of 4 hr, and impregnation ratio of 3:1 (acid/sample) The impregnated material filtered to remove excess acid and poured into a conical flask equipped in 700-watt power of microwave oven for activation under nitrogen flow of 150 cc/min with 20 min time of activation. The produced activated carbon was washed with hot water to remove the acid residue the washing water was tested for pH 6.5-7, and the activated carbon dried at 105˚C for 24 hr. In addition, the composite activated carbon was prepared by impregnating 25 g of AC in 250 ml of an aqueous suspension containing 1.25 g of SiO2 powder, and the resulting mixture was heated at 80 ^{o}C for 5 hours with 300 rpm stirring. The product was filtered, and the solid was washed with distilled water until the color in the residual liquid disappeared, then the solid product dried for 24 hours at 120 C, to obtain the desired adsorbent for the MG dye removal. SEM, and BET analyses were used to undertake the qualitative investigation of AC before adsorption.

3. Result and Discussion

3.1 Batch Experimental Studies

A batch experiment was proposed using the Taguchi method as described before and the response as experimental removal efficiency is illustrated in Table 3. The batch experiments were carried out to evaluate the factor's effects and their interaction on the removal efficiency of MG. 250mL Erlenmeyer flask containing the necessary adsorbent (0.1- 0.4) g/L of AC-SiO2 and (20-80) ppm of MG dye solution. The solution was agitated on a temperature-controlled mixer for a specified contact period (20-100) min. The mixture of AC-SiO2 and dye solution was filtered after specific time intervals to remove the solid from the solution. Ultraviolet-visible spectroscopy was used to determine the equilibrium concentration of MG

dye. The MG adsorption capacity and efficiency were determined in equations 1 and 2.

$q_e = (C_o - C_e)V/M$ …(1)

$RE\% = (C_o - C_e)/ C_o$ …(2)

Where C_o and C_e are dye initial and equilibrium concentrations (ppm), respectively; qe is the equilibrium capacity of MG (mg/g); V is the volume of MG solution (l); M is the mass of AC-SiO2 g).

Table 3,
Taguchi method for a batch design experiment

Ci	Time	Dosage	RE%
20	20	0.1	94.82%
20	40	0.2	95.39%
20	60	0.3	95.96%
20	100	0.4	96.53%
40	20	0.4	97.69%
40	40	0.3	97.98%
40	60	0.2	97.98%
40	100	0.1	97.41%
60	20	0.2	98.46%
60	40	0.1	98.65%
60	60	0.4	98.65%
60	100	0.3	98.27%
80	20	0.3	99.11%
80	40	0.4	99.13%
80	60	0.1	98.99%
80	100	0.2	98.70%

The final empirical formula (model) of MG removal efficiency AC-SiO2 (Y) was generated by the Taguchi method as shown in equation 3, which was well fitted with experimental data with $R^2 = 98.949556$.

$$Y = b_0 + b_1X_1 + b_2X_2 + b_3X_3 + b_{12}X_1X_2 + b_{13}X_1X_3 + b_{123}X_1X_2X_3 + b_{11}X_1^2 + b_{22}X_2^2 + b_{33}X_3^2 \quad \ldots(3)$$

where Y is the removal efficiency of MG, b0, b1, b2, and b3 are linear coefficients, b12, b13, and b123 are second-order interaction terms, and b11, b22, and b33 are quadratic terms of each factor X1, X2, and X3 are the coded phrases for MG concentration, mixing duration, and AC-SiO2 dosage. Tables 4 show the estimated values of the model coefficient, standard error of each model term, and p-value. It is obvious from the table that all coefficients have a substantial effect on model accuracy because their p-values are less than 0.05.

Table 4,
Model coefficients, standard error, and terms p- values for removal MG by AC-SiO2

Coefficient	Estimate	Standard error	t-value df=1	p-value	Lo.Conf Limit	Up.conf Limit
b0	0.904901	0.005904	9	0.011287	0.890456	0.919346
b1	0.001784	0.000163	1	0.016568	0.001386	0.002183
b2	0.000349	0.000111	1	0.013976	0.000078	0.000620
b3	0.062459	0.030699	1	0.022429	-0.012660	0.137578
b12	-0.000001	0.000157	1	0.025932	-0.000001	-0.000001
b13	-0.000286	0.000321	1	0.016033	-0.001073	0.000500
b123	-0.000006	0.000739	1	0.0221875	-0.000006	-0.000006
b11	-0.000010	0.000218	1	0.0186909	-0.000010	-0.000010
b22	-0.000002	0.000954	1	0.0198723	-0.000002	-0.000002

3.2 Adsorption Isotherm Model

Several adsorption isotherm models can be used to understand the behavior of adsorbate molecules at a solid-liquid contact. Langmuir (Langmuir 1916) examined adsorption data at a constant temperature using equation (4) to assume that adsorption is conducted as monolayer adsorption on homogeneous sites. Whereas Freundlich (Freundlich 1925). examined adsorption data at a constant temperature using equation (5) assuming that adsorption was conducted as multilayer adsorption on heterogeneous sites.

$$\frac{1}{q_e} = \frac{1}{q_m} + \frac{1}{k_L\, q_m\, c_e} \quad \ldots(4)$$

$$\ln q_e = \ln k_f + \left(\frac{1}{n}\right) \ln C_e \quad \ldots(5)$$

where q_e (mg/g) is the equilibrium adsorption capacity, and qm (mg/g) is the full monolayer adsorption capacity. Ce (mg/l) represents the equilibrium MG concentration, k_l (l/mg), k_f (l/mg) and 1/n are constants.

The adsorption behavior of MG on AC-SiO_2 was represented by Langmuir and Freundlich models as shown in Figures 2 and 3. It's noted from these Figures that the adsorption followed the Freundlich model (R^2 = 0.9906) which implies that the MG adsorption process occurred on the assumption of multilayer adsorption on the heterogeneous surface of AC-SiO_2. This behavior is similar to that reported by [41]. Table 5 summarizes the Langmuir and Freundlich coefficients that fitted with experimental data for malachite green (MG) adsorbed on AC-SiO_2.

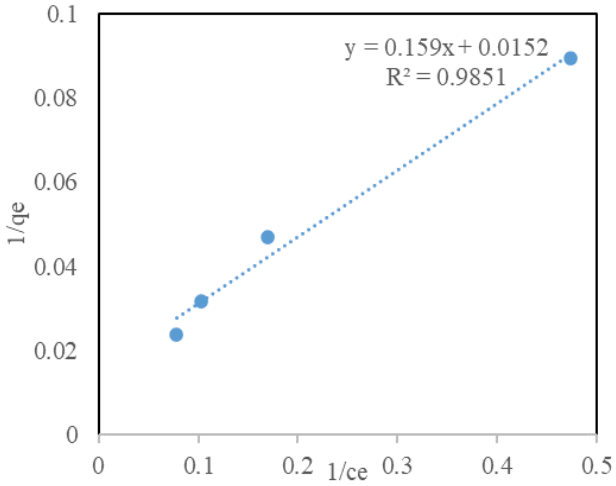

Fig. 2. Langmuir isotherm model for MG adsorption by AC-SiO2.

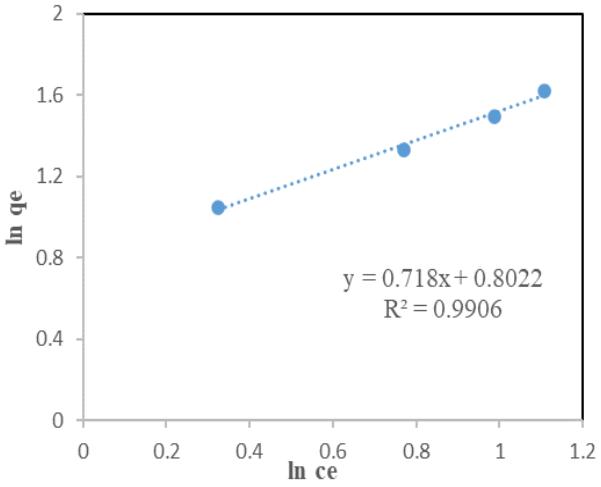

Fig. 3. Freundlich isotherm model for MG adsorption by AC-SiO_2.

Table 5,
Freundlich and Langmuir coefficients for MG adsorption on AC-SiO_2

Langmuir			Freundlich		
K_L (L/mg)	q_m (mg/g)	R^2	K_f (mg/g)	n	R^2
0.09551	65.7696	0.9851	2.2305	1.3927	0.9906

3.3 Kinetics of Adsorption

The adsorption process mechanism of MG on AC-SiO2 can be represented by several kinetic models. The pseudo-first-order and pseudo-second-order models as well-known models to observe the mechanism of the adsorption process as physisorption or chemisorption are represented by equations 6 and 7.

$$\ln(q_e - q_t) = \ln q_e - k_1 t \quad \ldots(6)$$

$$t/qt = (1/k_2 q_e^2) + (t/q_e) \quad \ldots(7)$$

where q_e (mg/g) is the equilibrium adsorption capacity, q_t (mg/g) is the adsorption capacity, t (min) is the time of adsorption, k_l (l/min) and k_2 (mg/g.min) are constants.

Figures 4 shows the plot of ln ($q_e - q_t$) versus time of adsorption (t) as a pseudo-first-order model as given in equation (5) with the value of model (R^2 = 0.9458) whereas Figure 5 shows the plots of t/q_t versus time of adsorption (t) as pseudo-second-order model as given in equation (6) with the value of model (R^2 = 0.9657). It's noted that the adsorption process is well-fitted with a pseudo-

second-order model which means that the mechanism of the adsorption process complied with chemisorption. This mechanism is similar to that reported by [42]. The kinetic parameters for two kinetic models and correlation coefficients were summarized in Table 6.

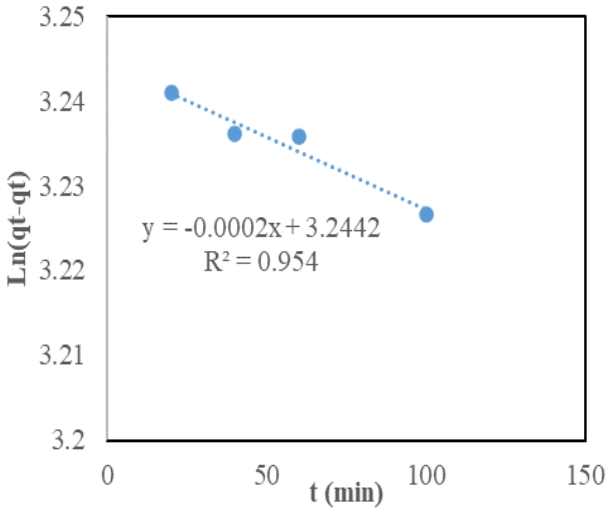

Fig. 4. Plots of pseudo-first-order adsorption kinetics of MG adsorption mechanism.

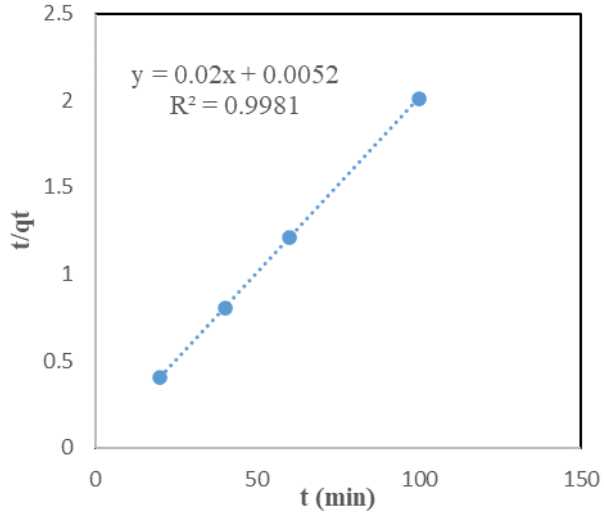

Fig. 5. Plots of pseudo-second-order adsorption kinetics of MG adsorption mechanism

Table 6,
The kinetic parameters for two kinetic model and correlation coefficients.

Pseudo-first order				Pseudo-second order			
qe, exp (mg/g)	K_1 (1/min)	qe,cal (mg/g)	R^2	K_2 (g/mg min)	qe, cal (mg/g)	R^2	
47.4356	0.00017	25. 641	0.9548	0.07707	49.9		0.9981

3.4 Adsorbent Characterization

3.4.1. Characterization using BET

Brunaure-Emmett-Teller technique (USA, HORIBA, SA-900 series) was used to determine the specific surface area of the activated carbon sample based on liquid nitrogen adsorption-desorption isotherm at temperature (77K), and the data obtained are summarized in Table 7.

Table 7,
BET analysis of AC

Sample weight	0.0255	[g]
Standard volume	9.779	[cm^3]
Dead volume	15.21	[cm^3]
Equilibrium time	0	[sec]
Adsorptive	N_2	
Apparatus temperature	0	[C]
Adsorption temperature	77.000	[K]
Saturated vapor pressure	84.772	[kPa]
Adsorption cross section area	0.162	[nm^2]

BET plot		
V_m	15.454	[cm^3(STP) g^{-1}]
$a_{s,BET}$	672.65	[m^2 g^{-1}]
C	66.879	
Total pore volume (p/p_0=0.990)	0.5889	[cm^3 g^{-1}]
Mean pore diameter	35.02	[nm]

The BET surface area of activated carbons treated with SiO_2 produced from Ficus Benjamin was found to be relatively high, with the optimal surface area being 672 m^2/g. The adsorption cross-section area of the sample is 0.162 nm^2 in the nanopore range. The average pore width was determined to be 35.025 nm, which corresponds to IUPAC categories of nanoporous materials within the given range [43].

3.4.2. Characterization using SEM

A scanning electron microscope was used to analyze the surface shape and topographical features (SEM). The generated photographs are three-dimensional and accurately depict the surface form. The Energy Dispersive X-ray Spectrophotometer is used to examine the AC/SiO_2 precursor elements (EDS). SEM-EDS analysis was performed using TESCAN, Vega III, Czech Republic. Figure 6 shows the morphology of the AC/SiO_2 precursor surface is not smooth and not homogeneous in appearance, with somewhat visible pores with a layered structure and spongy nature and various pores sizes and shapes. These holes' variability in sizes and shapes arose from the breakdown and volatilization of non-carbonaceous material in feedstock, and the pores generated as a result of chemical and physical activation provide dyes a good chance of being adsorbed. The white spot on the surface of the precursor is referred to SiO_2 which increases the surface area without blocking porosity, the presence of SiO_2 makes a thin layer on the surface of the AC which increases the curvature leading to an increase in the surface area.

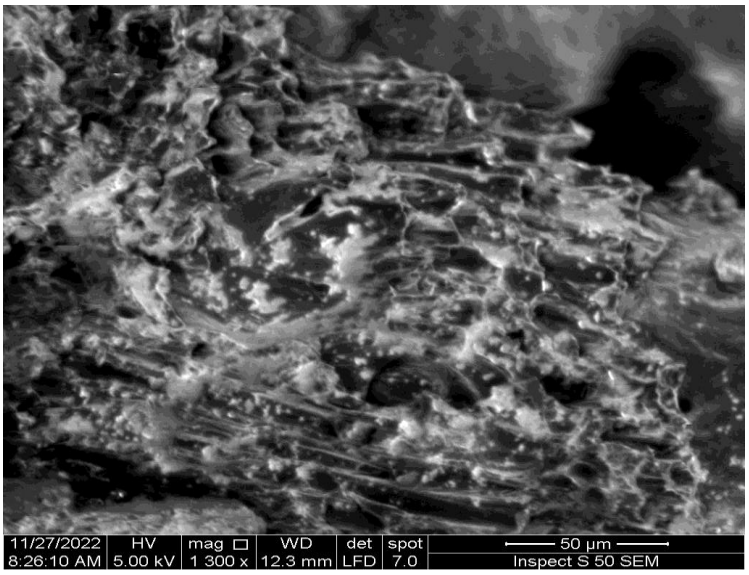

Fig. 6. SEM for AC.

3.4.3 Characterization using FTIR

Fourier Transform Infrared Spectroscopy was utilized to determine the functional groups that occur on the surface of both Ficus Benjamin and AC/SiO2. The infrared spectra were examined using a Fourier transform infrared spectrophotometer (IR Affinity-1 Shimadzu, Japan). Figure 7 (a, b) show the FTIR of AC used in the research.

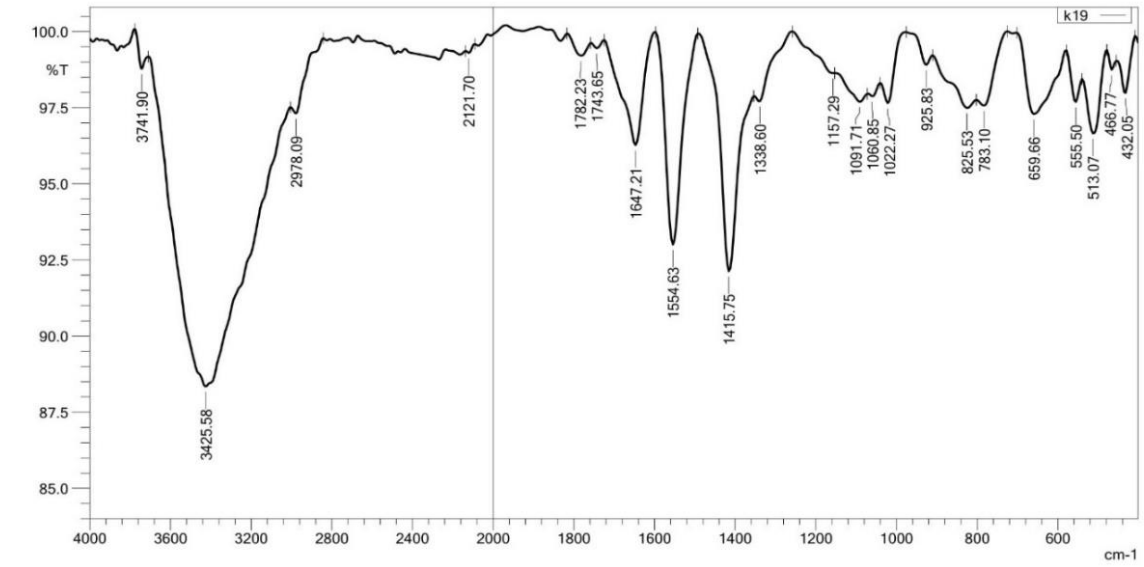

(a)

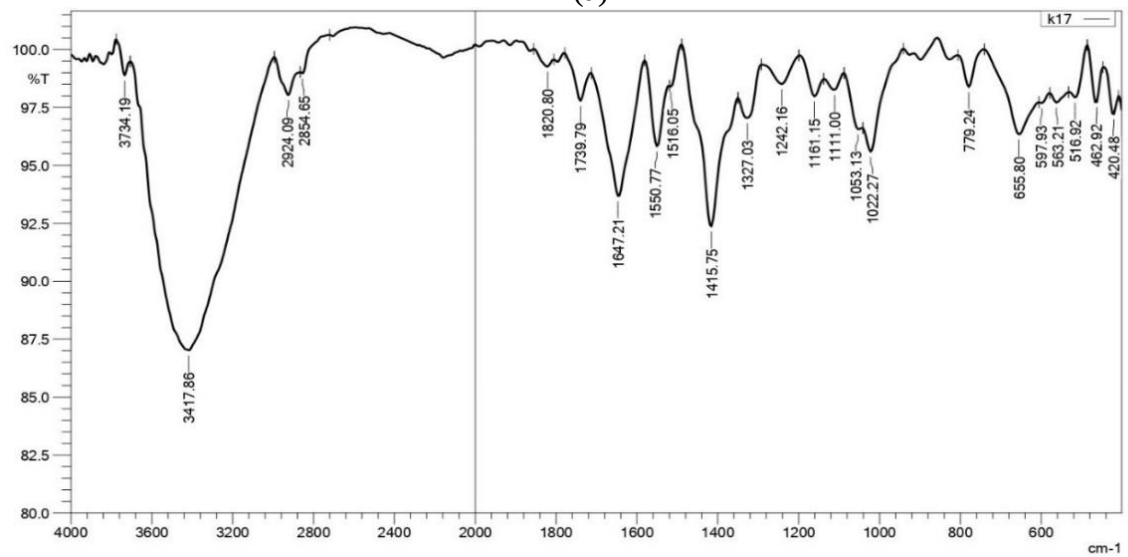

(b)

Fig. 7. a) FTIR for AC/SiO2, b) FTIR for Ficus Benjamin WOOD.

Ficus Benjamin and AC's FTIR spectra, as seen in Fig. 7 (a and b). It is obvious that the FTIR spectra of AC have lower intensities than the spectrum of Ficus Benjamin and that many of Ficus Benjamin's peaks have vanished. This evanescence is caused by the dissolution of chemical bonds during the H_3PO_4-impregnation, which then causes the carbonization process to eliminate and liberate a variety of volatile molecules [44]. The AC FTIR spectra revealed four peaks at 3425, 1647, 1554, and 1415 cm^{-1}. It is possible that the hydroxyl group of the O-H stretching vibration appears at 3425 cm^{-1} [45]. The peak of about 1554 cm^{-1} could be attributed to C=C stretching vibrations in the aromatic rings, and the band around 1647 cm^{-1} to CC stretching vibrations in the alkyne groups [46]. While the 1415 cm^{-1} peak shows the presence of C-O stretching vibrations in alcohols, phenols, acids, ethers, or esters [47].

3.5. Surface Analysis Response

The effect of MG concertation, time of mixing, and dose of adsorbent on removal efficiency at pH = 4 and mixing speed = 400 rpm are illustrated in 3D response surface plots as shown in Figure 8 and 9. Figure 8 depicts the effect of various initial concentrations of MG dye (20, 40, 60, and 80) mg/L with an adsorbent dose ranging from (0.1 - 0.4) g/50 ml. It's noted from this figure that the adsorption of MG dye increase as the adsorbate concentration increases until it reaches to surface saturated with adsorbate concentration (80 mg/L)

which means that the adsorbent has more free active sites on its surface to facilitate adsorption [19]. Likewise, as shown in Figure 9, the effect of MG concentration with various mixing time (20-100) min, as the time of mixing increased the removal efficiency increased before becoming constant at 80 mg/L which mean that the active site of the adsorbent saturated with MG particles [41].

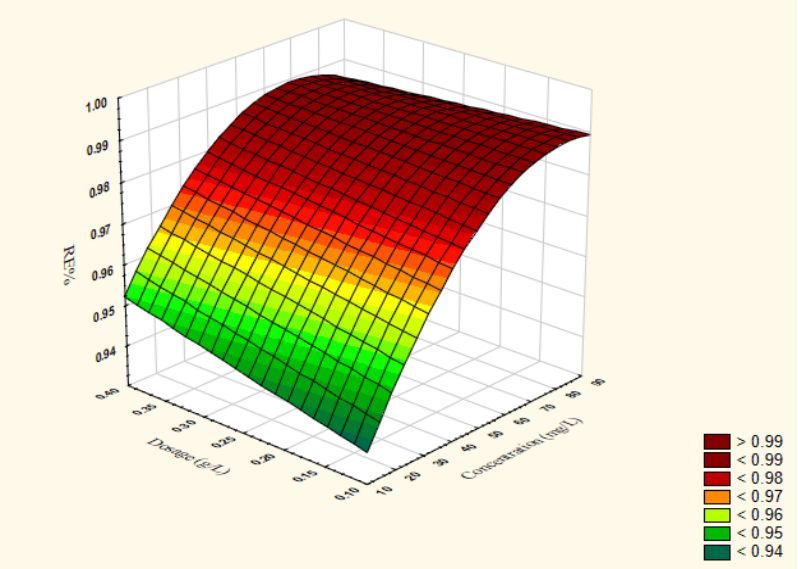

Fig. 8. removal efficiency of MG versus concentration and adsorbent dose.

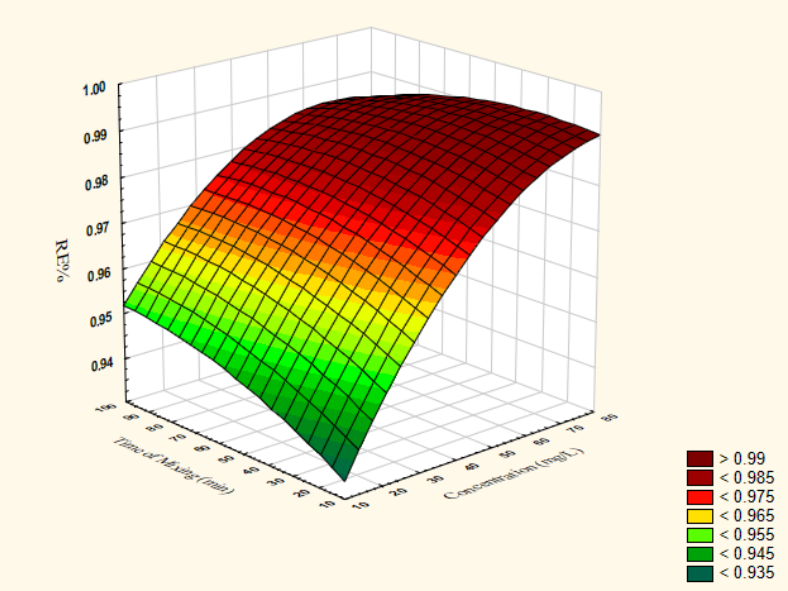

Fig. 9 Removal efficiency of MG versus concentration and time of mixing.

4. Conclusion

The present research revealed that Ficus Binjamina agro-waste can effectively be used as a raw material for the preparation of activated carbon pyro carbonic acid microwave method silicon oxide (SiO_2) as composite material for the removal of MG dye from aqueous solutions. The adsorption process followed the Freundlich and pseudo-second-order kinetic models which explained that the adsorption may involve multilayer adsorption behavior with interactions between the adsorbate molecules and the availability of the adsorbent sites than the adsorbate concentration. pesticides in

solution. The experiment conditions with the method of activation were optimized using the experimental design methodology and the results were analyzed with the STATISTICA 12.5 Software. The results of the adsorption studies show that the equilibrium of adsorption was reached in around 40 minutes, and the best adsorbent was discovered to be 80 mg/ L at pH 6 and a mixing speed 400 rpm. According to the desorption investigations, the malachite green was preferably adsorbed on the carbon surface in the presence of silicon oxide. As a result, wastewater from the textile and aquaculture industries can be treated with activated carbon derived from Ficus Binjamina agro-waste materials to eliminate malachite green.

Acknowledgments

The authors are grateful to the Biochemical Engineering Department, Al-Khwarizmi College of Engineering, University of Baghdad, for their support to carry out this research work.

5. References

[1] H. Sharifpour, N. Javid, and M. Malakootian, "Investigation of single-walled carbon nanotubes in removal of penicillin g (Benzyl penicillin sodium) from aqueous environments," *Desalin. Water Treat.*, vol. 124, pp. 248–255, Aug. 2018, doi: 10.5004/DWT.2018.22726.

[2] N. Javid, Z. Honarmandrad, and M. Malakootian, "Ciprofloxacin removal from aqueous solutions by ozonation with calcium peroxide," *Desalin. Water Treat.*, vol. 174, pp. 178–185, 2020, doi: 10.5004/dwt.2020.24855.

[3] A. H. Mahvi, M. Malakootian, and M. R. Heidari, "Comparison of polyaluminum silicate chloride and electrocoagulation process, in natural organic matter removal from surface water in Ghochan, Iran," *J. Water Chem. Technol.*, vol. 33, no. 6, pp. 377–385, Dec. 2011, doi: 10.3103/S1063455X11060051.

[4] M. Malakootian, N. Radhakrishna, M. P. Mazandarany, and H. Hossaini, "Bacterial-aerosol emission from wastewater treatment plant," *New pub Balaban*, vol. 51, no. 22–24, pp. 4478–4488, 2013, doi: 10.1080/19443994.2013.769668.

[5] X. Zheng *et al.*, "Overview of membrane technology applications for industrial wastewater treatment in China to increase water supply," *Resour. Conserv. Recycl.*, vol. 105, pp. 1–10, Dec. 2015, doi: 10.1016/J.RESCONREC.2015.09.012.

[6] S. Natarajan, H. C. Bajaj, and R. J. Tayade, "Recent advances based on the synergetic effect of adsorption for removal of dyes from waste water using photocatalytic process," *J. Environ. Sci.*, vol. 65, pp. 201–222, Mar. 2018, doi: 10.1016/J.JES.2017.03.011.

[7] E. A. Dil *et al.*, "Modeling of quaternary dyes adsorption onto ZnO–NR–AC artificial neural network: Analysis by derivative spectrophotometry," *J. Ind. Eng. Chem.*, vol. 34, pp. 186–197, Feb. 2016, doi: 10.1016/J.JIEC.2015.11.010.

[8] M. Abbas *et al.*, "Vibrio fischeri bioluminescence inhibition assay for ecotoxicity assessment: A review," *Sci. Total Environ.*, vol. 626, pp. 1295–1309, Jun. 2018, doi: 10.1016/J.SCITOTENV.2018.01.066.

[9] S. De Gisi, G. Lofrano, M. Grassi, and M. Notarnicola, "Characteristics and adsorption capacities of low-cost sorbents for wastewater treatment: A review," *Sustain. Mater. Technol.*, vol. 9, pp. 10–40, Sep. 2016, doi: 10.1016/J.SUSMAT.2016.06.002.

[10] M. Iqbal, M. Abbas, J. Nisar, A. Nazir, and A. Qamar, "Bioassays based on higher plants as excellent dosimeters for ecotoxicity monitoring: A review," *Chem. Int.*, vol. 5, no. 1, pp. 1–80, 2019.

[11] N. Mohammadi, H. Khani, V. K. Gupta, E. Amereh, and S. Agarwal, "Adsorption process of methyl orange dye onto mesoporous carbon material–kinetic and thermodynamic studies," *J. Colloid Interface Sci.*, vol. 362, no. 2, pp. 457–462, Oct. 2011, doi: 10.1016/J.JCIS.2011.06.067.

[12] R. Saravanan, S. Karthikeyan, V. K. Gupta, G. Sekaran, V. Narayanan, and A. Stephen, "Enhanced photocatalytic activity of ZnO/CuO nanocomposite for the degradation of textile dye on visible light illumination," *Mater. Sci. Eng. C*, vol. 33, no. 1, pp. 91–98, Jan. 2013, doi: 10.1016/J.MSEC.2012.08.011.

[13] M. Malakootian, A. Nasiri, A. Asadipour, and E. Kargar, "Facile and green synthesis of ZnFe2O4@CMC as a new magnetic nanophotocatalyst for ciprofloxacin degradation from aqueous media," *Process Saf. Environ. Prot.*, vol. 129, pp. 138–151, Sep. 2019, doi: 10.1016/J.PSEP.2019.06.022.

[14] A. Kausar *et al.*, "Dyes adsorption using clay and modified clay: A review," *J. Mol. Liq.*, vol. 256, pp. 395–407, Apr. 2018, doi: 10.1016/J.MOLLIQ.2018.02.034.

[15] V. Katheresan, J. Kansedo, and S. Y. Lau, "Efficiency of various recent wastewater dye removal methods: A review," *J. Environ. Chem. Eng.*, vol. 6, no. 4, pp. 4676–4697, Aug. 2018, doi: 10.1016/J.JECE.2018.06.060.

[16] A. Saravanan *et al.*, "Phytoremediation of Cr(VI) ion contaminated soil using Black gram (Vigna mungo): Assessment of removal capacity," *J. Environ. Chem. Eng.*, vol. 7, no. 3, p. 103052, Jun. 2019, doi: 10.1016/J.JECE.2019.103052.

[17] L. Gan, F. Zhou, G. Owens, and Z. Chen, "Burkholderia cepacia immobilized on eucalyptus leaves used to simultaneously remove malachite green (MG) and Cr(VI)," *Colloids Surfaces B Biointerfaces*, vol. 172, pp. 526–531, Dec. 2018, doi: 10.1016/J.COLSURFB.2018.09.008.

[18] A. A. El-Zahhar and N. S. Awwad, "Removal of malachite green dye from aqueous solutions using organically modified hydroxyapatite," *J. Environ. Chem. Eng.*, vol. 4, no. 1, pp. 633–638, Mar. 2016, doi: 10.1016/J.JECE.2015.12.014.

[19] T. R. Sundararaman *et al.*, "Adsorptive Removal of Malachite Green Dye onto Coal-Associated Soil and Conditions Optimization," *Adsorpt. Sci. Technol.*, vol. 2021, 2021, doi: 10.1155/2021/5545683.

[20] F. Jiang, D. M. Dinh, and Y. Lo Hsieh, "Adsorption and desorption of cationic malachite green dye on cellulose nanofibril aerogels," *Carbohydr. Polym.*, vol. 173, pp. 286–294, Oct. 2017, doi: 10.1016/J.CARBPOL.2017.05.097.

[21] S. Hajialigol and S. Masoum, "Optimization of biosorption potential of nano biomass derived from walnut shell for the removal of Malachite Green from liquids solution: Experimental design approaches," *J. Mol. Liq.*, vol. 286, p. 110904, Jul. 2019, doi: 10.1016/J.MOLLIQ.2019.110904.

[22] S. Jeevanantham, A. Saravanan, R. V. Hemavathy, P. S. Kumar, P. R. Yaashikaa, and D. Yuvaraj, "Removal of toxic pollutants from water environment by phytoremediation: A survey on application and future prospects," *Environ. Technol. Innov.*, vol. 13, pp. 264–276, Feb. 2019, doi: 10.1016/J.ETI.2018.12.007.

[23] V. Tharaneedhar, P. Senthil Kumar, A. Saravanan, C. Ravikumar, and V. Jaikumar, "Prediction and interpretation of adsorption parameters for the sequestration of methylene blue dye from aqueous solution using microwave assisted corncob activated carbon," *Sustain. Mater. Technol.*, vol. 11, pp. 1–11, Apr. 2017, doi: 10.1016/J.SUSMAT.2016.11.001.

[24] A. E. Burakov *et al.*, "Adsorption of heavy metals on conventional and nanostructured materials for wastewater treatment purposes: A review," *Ecotoxicol. Environ. Saf.*, vol. 148, pp. 702–712, Feb. 2018, doi: 10.1016/J.ECOENV.2017.11.034.

[25] Suhas, V. K. Gupta, P. J. M. Carrott, R. Singh, M. Chaudhary, and S. Kushwaha, "Cellulose: A review as natural, modified and activated carbon adsorbent," *Bioresour. Technol.*, vol. 216, pp. 1066–1076, Sep. 2016, doi: 10.1016/J.BIORTECH.2016.05.106.

[26] A. Saravanan, S. Jeevanantham, P. Senthil Kumar, S. Varjani, P. R. Yaashikaa, and S. Karishma, "Enhanced Zn(II) ion adsorption on surface modified mixed biomass – Borassus flabellifer and Aspergillus tamarii: Equilibrium, kinetics and thermodynamics study," *Ind. Crops Prod.*, vol. 153, p. 112613, Oct. 2020, doi: 10.1016/J.INDCROP.2020.112613.

[27] S. Sadaf, H. N. Bhatti, S. Nausheen, and M. Amin, "Application of a novel lignocellulosic biomaterial for the removal of Direct Yellow 50 dye from aqueous solution: Batch and column study," *J. Taiwan Inst. Chem. Eng.*, vol. 47, pp. 160–170, Feb. 2015, doi: 10.1016/J.JTICE.2014.10.001.

[28] M. M. Meimand, N. Javid, and M. Malakootian, "Adsorption of Sulfur Dioxide on Clinoptilolite/Nano Iron Oxide and Natural Clinoptilolite," *Heal. Scope 2019 82*, vol. 8, no. 2, Mar. 2019, doi: 10.5812/JHEALTHSCOPE.69158.

[29] F. Nekouei, S. Nekouei, I. Tyagi, and V. K. Gupta, "Kinetic, thermodynamic and isotherm studies for acid blue 129 removal from liquids using copper oxide nanoparticle-modified activated carbon as a novel adsorbent," *J. Mol. Liq.*, vol. 201, pp. 124–133, Jan. 2015, doi: 10.1016/J.MOLLIQ.2014.09.027.

[30] S. Suganya, P. Senthil Kumar, A. Saravanan, P. Sundar Rajan, and C. Ravikumar, "Computation of adsorption parameters for the removal of dye from wastewater by microwave assisted sawdust: Theoretical and experimental analysis," *Environ. Toxicol. Pharmacol.*, vol. 50, pp. 45–57, Mar. 2017, doi: 10.1016/J.ETAP.2017.01.014.

[31] L. Lin, S. Tang, X. Wang, X. Sun, and A. Yu, "Adsorption of malachite green from aqueous solution by nylon microplastics: Reaction mechanism and the optimum conditions by response surface methodology," *Process Saf. Environ. Prot.*, vol. 140, pp. 339–347, Aug. 2020, doi: 10.1016/J.PSEP.2020.05.019.

[32] F. Bouaziz, M. Koubaa, F. Kallel, R. E. Ghorbel, and S. E. Chaabouni, "Adsorptive removal of malachite green from aqueous solutions by almond gum: Kinetic study and equilibrium isotherms," *Int. J. Biol. Macromol.*, vol. 105, pp. 56–65, Dec. 2017, doi: 10.1016/J.IJBIOMAC.2017.06.106.

[33] J. Wu, J. Yang, P. Feng, G. Huang, C. Xu, and B. Lin, "High-efficiency removal of dyes from wastewater by fully recycling litchi peel biochar," *Chemosphere*, vol. 246, p. 125734, May 2020, doi: 10.1016/J.CHEMOSPHERE.2019.125734.

[34] P. Geetha, M. S. Latha, and M. Koshy, "Biosorption of malachite green dye from aqueous solution by calcium alginate nanoparticles: Equilibrium study," *J. Mol. Liq.*, vol. 212, pp. 723–730, Dec. 2015, doi: 10.1016/J.MOLLIQ.2015.10.035.

[35] S. Banerjee, G. C. Sharma, R. K. Gautam, M. C. Chattopadhyaya, S. N. Upadhyay, and Y. C. Sharma, "Removal of Malachite Green, a hazardous dye from aqueous solutions using Avena sativa (oat) hull as a potential adsorbent," *J. Mol. Liq.*, vol. 213, pp. 162–172, Jan. 2016, doi: 10.1016/J.MOLLIQ.2015.11.011.

[36] H. A. Chanzu, J. M. Onyari, and P. M. Shiundu, "Brewers' spent grain in adsorption of aqueous Congo Red and malachite Green dyes: Batch and continuous flow systems," *J. Hazard. Mater.*, vol. 380, p. 120897, Dec. 2019, doi: 10.1016/J.JHAZMAT.2019.120897.

[37] E. Mkrtchyan, A. Burakov, and I. Burakova, "The Adsorption of Malachite Green on Graphene Nanocomposites: A Study on Kinetics Under Dynamic Conditions," *Mater. Today Proc.*, vol. 11, pp. 404–409, Jan. 2019, doi: 10.1016/J.MATPR.2019.01.004.

[38] P. Saha, S. Chowdhury, S. Gupta, and I. Kumar, "Insight into adsorption equilibrium, kinetics and thermodynamics of Malachite Green onto clayey soil of Indian origin," *Chem. Eng. J.*, vol. 165, no. 3, pp. 874–882, Dec. 2010, doi: 10.1016/J.CEJ.2010.10.048.

[39] B. QU, J. ZHOU, X. XIANG, C. ZHENG, H. ZHAO, and X. ZHOU, "Adsorption behavior of Azo Dye C. I. Acid Red 14 in aqueous solution on surface soils," *J. Environ. Sci.*, vol. 20, no. 6, pp. 704–709, Jan. 2008, doi: 10.1016/S1001-0742(08)62116-6.

[40] J. B. Tarkwa *et al.*, "Highly efficient degradation of azo dye Orange G using laterite soil as catalyst under irradiation of non-thermal plasma," *Appl. Catal. B Environ.*, vol. 246, pp. 211–220, Jun. 2019, doi: 10.1016/J.APCATB.2019.01.066.

[41] I. A. Rahman, B. Saad, S. Shaidan, and E. S. Sya Rizal, "Adsorption characteristics of malachite green on activated carbon derived from rice husks produced by chemical–thermal process," *Bioresour. Technol.*, vol. 96, no. 14, pp. 1578–1583, Sep. 2005, doi: 10.1016/J.BIORTECH.2004.12.015.

[42] Y. Önal, C. Akmil-Başar, D. Eren, Ç. Sarici-Özdemir, and T. Depci, "Adsorption kinetics of malachite green onto activated carbon prepared from Tunçbilek lignite," *J. Hazard. Mater.*, vol. 128, no. 2–3, pp. 150–157, Feb. 2006, doi: 10.1016/J.JHAZMAT.2005.07.055.

[43] B. D. Zdravkov, J. J. Čermák, M. Šefara, and J. Janků, "Pore classification in the characterization of porous materials: A perspective," *Cent. Eur. J. Chem.*, vol. 5, no. 2, pp. 385–395, Jun. 2007, doi: 10.2478/S11532-007-0017-9/MACHINEREADABLECITATION/RIS.

[44] E. Yagmur, M. Ozmak, and Z. Aktas, "A novel method for production of activated carbon from waste tea by chemical activation with microwave energy," *Fuel*, vol. 87, no. 15–16, pp. 3278–3285, Nov. 2008, doi: 10.1016/J.FUEL.2008.05.005.

[45] B. H. Hameed, J. M. Salman, and A. L. Ahmad, "Adsorption isotherm and kinetic modeling of 2 , 4-D pesticide on activated carbon derived from date stones," vol. 163, pp. 121–126, 2009, doi: 10.1016/j.jhazmat.2008.06.069.

[46] J. Yang and K. Qiu, "Development of high surface area mesoporous activated carbons from herb residues," *Chem. Eng. J.*, vol. 167, no. 1, pp. 148–154, Feb. 2011, doi: 10.1016/J.CEJ.2010.12.013.

[47] W. Tongpoothorn, M. Sriuttha, P. Homchan, S. Chanthai, and C. Ruangviriyachai, "Preparation of activated carbon derived from Jatropha curcas fruit shell by simple thermo-chemical activation and characterization of their physico-chemical properties," *Chem. Eng. Res. Des.*, vol. 89, no. 3, pp. 335–340, Mar. 2011, doi: 10.1016/J.CHERD.2010.06.012.

إزالة صبغة الملكيت الأخضر من المحلول المائي باستخدام أكسيد الكربون اللافلزي المنشط من نبات الفيكس بنجامينا الذي تم تصنيعه بواسطة الميكروويف مع حمض الكربونيك

خطاب عماد طالب* سامي داود سلمان**

*،**قسم الهندسة الكيميائية الاحيائية/ كلية الهندسة الخوارزمي/ جامعة بغداد

*البريد الالكتروني:khattab.i@kecbu.uobaghdad.edu.iq

**البريد الالكتروني:sami.albayati@gmail.com

الخلاصة

تم استخدام الكربون المنشط المشتق من المخلفات الزراعية لنبتة الفيكس بنجامينا الزراعية والمُصنَّع بواسطة طريقة الميكروويف مع حمض الفسفوريك ومعالجته بأوكسيد السيليكون (SiO_2) لتعزيز قدرة الكاربون المنشط لامتزاز لصبغة الملكيت الأخضر (MG) من المحلول المائي. تم دراسة ثلاثة عوامل بأربعة مستويات للتحقق من تأثيرها على كفاءة أزالة الصبغة الملكيت الأخضر من المحلول المائي منها تركيز الصبغة، وقت الخلط وكمية الكربون المنشط. أظهرت النتائج أن جرعة 0.4 جم / لتر، تركيز صبغة 80 مجم / لتر، ومدة امتصاص 40 دقيقة كشرط أمثل للوصول الى كفاءة الإزالة بحدود 99.13٪. وقد كشفت النتائج أيضًا أن نموذج التوازن الحراري فروندليتش فضلا عن النماذج الحركية الزائفة من الدرجة الثانية كانت أفضل النماذج لوصف بيانات امتزاز صبغة الملكيت الأخضر عند التوازن.